Chapter 15
Age-Specific Mortality and Fertility Rates for Probabilistic Population Projections

Hana Ševčíková, Nan Li, Vladimíra Kantorová, Patrick Gerland, and Adrian E. Raftery

15.1 Introduction

Projections of countries' future populations, broken down by age and sex, are used by governments for social, economic and infrastructure planning, by international organizations for development planning and monitoring and global modeling, by the private sector for strategic and marketing decisions, and by academic and other researchers as inputs to social and health research.

Most population projections have until recently been done deterministically, using the cohort component method (Whelpton 1928, 1936). This is an age- and sex-structured version of the basic demographic identity that the population of a country at the next time point is equal to the population at the current time point, plus the number of births, minus the number of deaths, plus the number of immigrants minus the number of emigrants. It was formulated in matrix form by Leslie (1945) and is described in detail in Preston et al. (2001, Chap. 6).

Population projections are currently produced by many organizations, including national and local governments and private companies. The main organizations that have produced population projections for all or most of the world's countries are the United Nations (UN) (United Nations 2011), the World Bank (Bos et al. 1994),

H. Ševčíková
Center for Statistics and the Social Sciences, University of Washington, Seattle, WA 98195-4320, USA
e-mail: hanas@u.washington.edu

N. Li • V. Kantorová • P. Gerland
United Nations Population Division, United Nations, New York, NY 10017, USA
e-mail: li32@un.org; kantorova@un.org; gerland@un.org

A.E. Raftery (✉)
Departments of Statistics and Sociology, University of Washington, Seattle, WA 98195-4322, USA
e-mail: raftery@u.washington.edu

R. Schoen (ed.), *Dynamic Demographic Analysis*,
The Springer Series on Demographic Methods and Population Analysis 39,
DOI 10.1007/978-3-319-26603-9_15

and the United States Census Bureau (U. S. Census Bureau 2009), all of which have until recently used the standard deterministic approach. Among these, the UN produces updated projections for all the world's countries every 2 years, published as the *World Population Prospects*, and these are the de facto standard (Lutz and Samir 2010).

Standard population projection methods are deterministic, meaning that they yield a single projected value for each quantity of interest. However, probabilistic projections that give a probability distribution of each quantity of interest, and hence convey uncertainty about the projections, are widely desired. They are needed for planning purposes. For example, those planning school construction may wish to be reasonably sure of building enough capacity to accommodate all students in the future. For this the relevant projection is an upper quantile of the predictive distribution of the future school population that is relatively unlikely to be exceeded, rather than a "best guess." Probabilistic projections are also useful for assessing change and deviations of population outcomes from expectations, as well as for providing a general assessment of uncertainty about future population.

The most common approach to communicating uncertainty in population projections has been the scenario, or High-Medium-Low, approach. In this approach, a central or main projection is first produced. Then high and low values of the main inputs to the projection model, such as fertility or mortality, are postulated, and a projection is produced with the high values, and another one with the low values. These high and low trajectories are viewed as bracketing the likely future values. This approach has been criticized as having no probabilistic basis and leading to inconsistencies (Lee and Tuljapurkar 1994; National Research Council 2000).

Previous approaches to producing probabilistic population projections include ex-post analysis, time series methods and expert-based approaches (National Research Council 2000; Booth et al. 2006). Ex-post analysis is based on the errors in past forecasts (Keyfitz 1981; Stoto 1983; Alho et al. 2006, 2008; Alders et al. 2007). The time-series analysis approach uses past time series of forecast inputs, such as fertility and mortality, to estimate a statistical time series model, which is then used to simulate a large number of random possible future trajectories. Simulated trajectories of forecast inputs are combined via a cohort component projection model to produce predictive distributions of forecast outputs (Lee and Tuljapurkar 1994; Tuljapurkar and Boe 1999). In the expert-based method (Pflaumer 1988; Lutz et al. 1996, 1998, 2004) experts are asked to provide distributions for each forecast input. These are then used to construct predictive distributions of forecast outputs using a stochastic method similar to the time series method.

The United Nations released official probabilistic population projections for all countries for the first time in July 2014 (Gerland et al. 2014). They were produced by probabilistically projecting the period total fertility rates (TFR) and life expectancies (e_0) for all countries using Bayesian hierarchical models (Alkema et al. 2011; Raftery et al. 2013). These probabilistic projections took the form of a large set of trajectories, each of which was sampled from the joint predictive distribution

of TFR and female and male e_0 for all countries and all future time periods to 2100 using Markov chain Monte Carlo (MCMC) methods.[1] Among previous probabilistic methods, the UN approach is most closely related to the time series approach.

For each trajectory, the life expectancies were converted to age- and sex-specific mortality rates, and the total fertility rates were converted to age-specific fertility rates. The population was then projected forward using the cohort-component method. This yielded a large set of trajectories of population by age and sex, and age-specific fertility and mortality rates, for all countries and future time periods jointly. These were summarized by predictive medians and 80 % and 95 % prediction intervals for a wide range of population quantities of interest, for all countries and a wide range of regional and other aggregates. They were published as the UN's Probabilistic Population Projections (PPP), and are available at http://esa.un.org/unpd/wpp.

This chapter focuses on the methods used to convert probabilistic projections of e_0 and TFR to probabilistic projections of age-specific mortality and fertility rates. Some limitations of the methods used for the 2014 PPP are identified, and several improvements are proposed to overcome them. The methods presented in this chapter are implemented in an open source R package called `bayesPop` (Ševčíková and Raftery 2014; Ševčíková et al. 2014).

The chapter is organized as follows. In Sect. 15.2 we describe the current method in PPP for projecting age-specific mortality rates, and our proposed improvements. In Sect. 15.2.1 we outline the Probabilistic Lee-Carter method used in the 2014 PPP. In the rest of Sect. 15.2 we propose several improvements to overcome limitations of this method. These include a new Coherent Kannisto Method for joint projection of future age-specific mortality rates at very high ages that avoids unrealistic crossovers between the sexes (Sect. 15.2.2), application of the Coherent Lee-Carter method to avoid crossovers at lower ages (Sect. 15.2.3), new methods for avoiding jump-off bias (Sect. 15.2.4), and application of the Rotated Lee-Carter method to reflect the fact that when mortality rates are low, they tend to decline faster at older than at younger ages (Sect. 15.2.5). In Sect. 15.3, we describe the current method in PPP for projecting age-specific fertility rates and our proposed improvements. We conclude with a discussion in Sect. 15.4.

[1]This general approach applies to countries experiencing normal mortality trends. For countries having ever experienced 2 % or more adult HIV prevalence during the period 1980–2010, all projected trajectories of life expectancy by sex for each of these countries were adjusted in such a way as to ensure that the median trajectory for each country was consistent with the 2012 Revision of the World Population Prospects deterministic projection that incorporates the impact of HIV/AIDS on mortality, as well as assumptions about future potential improvements both in the reduction of the epidemic and survival due to treatment.

15.2 Age-Specific Mortality Rates for Probabilistic Population Projections

15.2.1 Probabilistic Lee-Carter Method

Our methodology is based on the Lee-Carter model (Lee and Carter 1992). This was originally developed for a single country, and is defined as follows:

$$\log[m_x(t)] = a_x + b_x k(t) + \varepsilon_x(t), \quad \varepsilon_x(t) \sim N(0, \sigma_\varepsilon^2),$$

where $m_x(t)$ is the mortality rate for age x and time period t, the quantity a_x represents the baseline pattern of mortality by age over time, and b_x is the average rate of change in mortality rate by age group for a unit change in the mortality index $k(t)$. The parameter $k(t)$ is a time-varying index of the overall level of mortality, and $\varepsilon_x(t)$ is the residual at age x and time t. Throughout this chapter, log denotes the natural logarithm.

For a given matrix of rates $m_x(t)$, the model is estimated by a least squares method. The baseline mortality pattern a_x is estimated as the average of $\log[m_x(t)]$ over the past time periods with observed data. Since the model is underdetermined, b_x is identified by setting $\sum_x b_x = 1$, where the sum is over all ages or age groups x. Also, $k(t)$ is identified by setting $\sum_{t=1}^{T} k(t) = 0$, where T is the number of past time periods for which data are available. The estimates are then

$$\hat{a}_x = \frac{\sum_{t=1}^{T} \log[m_x(t)]}{T}, \tag{15.1}$$

$$\hat{k}(t) = \sum_x \{\log[m_x(t)] - \hat{a}_x\}, \tag{15.2}$$

$$\hat{b}_x = \frac{\sum_{t=1}^{T} \{\log[m_x(t)] - \hat{a}_x\}\, \hat{k}(t)}{\sum_{t=1}^{T} \hat{k}(t)^2}. \tag{15.3}$$

To forecast $m_x(t)$, one needs to project $k(t)$ into the future. To project $k(t)$, the Lee-Carter method uses a random walk with a constant drift d per time period, leading to the deterministic projections

$$\hat{k}(t+1) = \hat{k}(t) + \hat{d}, \quad \text{where } \hat{d} = \frac{1}{T-1}[\hat{k}(T) - \hat{k}(1)].$$

Lee and Miller (2001) proposed replacing the step of projecting $k(t)$ by itself by matching future $k(t)$ to future projected $e_0(t)$.

Current calculations are done using a highest age or open interval of 85+. For projections one needs to extend mortality rates to higher ages x, usually beyond 100+, because mortality rates are expected broadly to decline over time in the future, so there will be larger numbers of people at higher ages. For extending the

force of mortality at older age groups, the Kannisto model provides a simple but well-fitting way to approximate available mortality rates from age 80 to 100, and to extrapolate mortality rates up to age 130 in a way that is consistent with empirical observations on oldest-old mortality (Thatcher et al. 1998).

The Bayesian probabilistic projections of life expectancy at birth (Raftery et al. 2013, 2014b) provide us with a set of future trajectories of female and male e_0, representing a sample from the joint predictive distribution of future female and male e_0 for all countries and all future time periods. The 2014 PPP used methods for turning a trajectory of future e_0 values into a set of future age-specific mortality based on the ideas of Lee and Miller (2001) and Li and Gerland (2011); see Raftery et al. (2012). They were based on the following algorithm:

Algorithm 15.1

Let $t \in \{1, \ldots, T\}$ and $\tau \in \{T+1, \ldots, T_p\}$ denote the observed and projected time periods, respectively.

1. Using the Kannisto method extend $m_x(t)$ to higher age groups so that $\max(x) = 130+$ for all t.
2. Estimate a_x, $k(t)$ and b_x using the extended historical $m_x(t)$ (Eqs. (15.1), (15.2) and (15.3)), yielding estimates $\hat{a}_x$ and $\hat{b}_x$ for all age groups x.
3. For a given $e_0(\tau)$ in each trajectory and the estimates $\hat{a}_x$ and $\hat{b}_x$ from the previous step, solve for future $k(\tau)$ numerically using life tables. This yields a nonlinear equation which can be solved using the bisection method. More details are given in Sect. 15.2.6.
   This gives a sample of values of $k(\tau)$ for each future time period τ, with one value for each trajectory.
4. Compute age-specific mortality rates by $\log[m_x(\tau)] = \hat{a}_x + \hat{b}_x k(\tau)$ for each trajectory and future time period τ.

Applying these steps to all trajectories of e_0 yields a posterior predictive distribution of $m_x(t)$. Note that in the above algorithm, $k(\tau)$ is trajectory-specific, while $\hat{a}_x$ and $\hat{b}_x$ are the same for all trajectories.

However, this procedure has a number of drawbacks. There is no assurance that the extension of $m_x(t)$ to higher ages yields mortality rates that are coherent between males and females. Similarly, the predicted $m_x(\tau)$ can lead to unwanted crossovers between female and male mortality rates, since they are obtained independently for each sex. In the following sections, we present solutions to these and other limitations of the simple algorithm above, and give more details about Step 3.

15.2.2 Coherent Kannisto Method

A sex-independent extension of the observed mortality rates to higher age categories can lead to unrealistic crossovers at higher ages. We propose a modification of the Kannisto method that treats male and female mortality rates jointly. For simplicity we omit the time index t in this section.

The original Kannisto model has the form

$$m_x = \frac{ce^{dx}}{1 + ce^{dx}} e^{\varepsilon_x}, \quad \text{or}$$
$$\text{logit}(m_x) = \log c + dx + \varepsilon_x,$$

where ε_x is a random perturbation with mean zero. The model is usually estimated independently for each sex, assuming independence across ages and normality of the ε_x, using a maximum likelihood method (Thatcher et al. 1998; Wilmoth et al. 2007). This yields sex-specific parameter estimates $\hat{d}_M$, $\hat{d}_F$, $\hat{c}_M$, $\hat{c}_F$.

We suggest modifying this by forcing the sex-specific parameters d_M and d_F to be equal (i.e. $d_M = d_F = d$), but still allowing the parameters c_M and c_F to differ between the sexes:

$$\text{logit}(m_x^g) = \log c_g + dx + \varepsilon_x^g, \quad \text{for } g = M, F.$$

This leads to the following model:

$$\text{logit}(m_x^g) = \beta_0 + \beta_1 1_{(g=M)} + \beta_2 x + \varepsilon_x^g,$$

where $1_{(g=M)} = 1$ if $g = M$ and 0 otherwise.

To estimate the β parameters, we fit the model to the observed m_x for ages 80–99 by ordinary least-squares regression, which corresponds to maximum likelihood under the assumptions that the ε_x^g are independent and normally distributed and have the same variance. There are four age groups in the data used for fitting the model, and thus eight points in total for both sexes. Then,

$$\hat{c}_F = e^{\hat{\beta}_0},$$
$$\hat{c}_M = e^{\hat{\beta}_0 + \hat{\beta}_1},$$
$$\hat{d} = \hat{\beta}_2.$$

Figure 15.1 shows the resulting m_x for old ages for Brazil and Lithuania in the last observed time period. From the left panels we see that there are crossovers using the classic Kannisto method, which is unrealistic. However, male mortality stays above female mortality in the coherent version, as can be seen in the right panels; this is more realistic.

15.2.3 Coherent Lee-Carter Method

We adopt an extension of the Lee-Carter method suggested by Li and Lee (2005), the so-called *coherent* Lee-Carter method. It takes into account the fact that mortality patterns for closely related populations are expected to be similar. In our application,

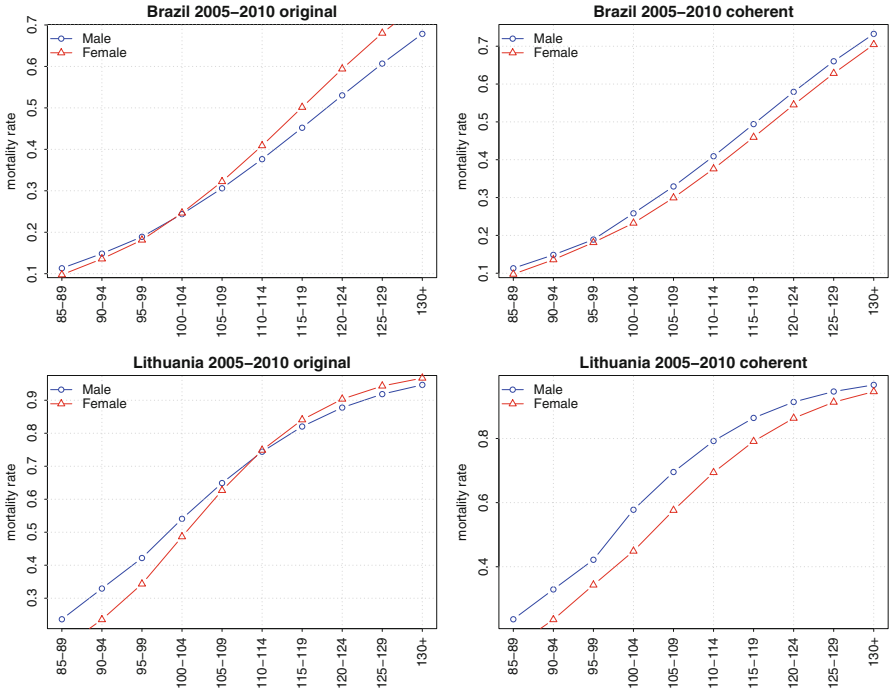

Fig. 15.1 Mortality rates for males and females extended using the coherent Kannisto method (*right panels*), compared to the original Kannisto method (*left panels*) for Brazil and Lithuania in the last observed time period (2005–2010)

these related populations will be males and females in the same country, since there is no expectation that the life expectancy will diverge between these groups. Thus, the Lee-Carter method is extended by two requirements:

$$\begin{aligned} b_x^M &= b_x^F, \\ k_M(\tau) &= k_F(\tau), \end{aligned} \tag{15.4}$$

where M and F denotes male and female sex, respectively. This ensures that the rates of change of the future mortality rates are the same for the two sexes, and thus avoids crossovers.

15.2.4 Avoiding Jump-Off Bias

Mortality rates in the last period of the historical data used for estimation (or jump-off period) are commonly referred to as jump-off rates (Booth et al. 2006). Often there is a mismatch between fitted rates for the last period T and the actual rates

(jump-off bias). As a result, a discontinuity between the actual rates in the jump-off period and the rates projected in the first projection period may occur.

A possible solution to avoid jump-off bias is to constrain the model in such a way that $k(t)$ passes through zero in the jump-off period T, and to use m_x only from the last fitting period to obtain a_x (Lee and Miller 2001):

$$a_x = \log[m_x(T)] \implies k(T) = 0. \tag{15.5}$$

A disadvantage of this solution is that in cases where the mortality rates are bumpy in the jump-off period (i.e. not smooth across ages), this "bumpiness" propagates into the future. In general for projections, we suggest using the age-specific mortality rates from the last fitting period and smoothing them over age if necessary (e.g. for small populations with few deaths in some age groups) while preserving the value for the youngest age group:

$$a_x = \text{smooth}_x\{\log[m_x(T)]\}, \text{ with } a_{0-1} = \log[m_{0-1}(T)]. \tag{15.6}$$

Figure 15.2 shows the resulting difference in $\log[m_x(\tau)]$ projected to τ corresponding to 2095–2100 for two countries using the three different methods of computing a_x, namely Eqs. (15.1), (15.5) and (15.6). As can be seen in the case of Bangladesh, the smoothing step removes bumps whereas the averaging method does not.

Figure 15.3 shows the impact of the methods on m_x as time series for Bangladesh for three different age groups. Using the average m_x results in jump-offs for the 5–9 and 95–99 age groups. If the latest raw m_x are used, the jump-offs are eliminated. A smoothed version creates a new jump-off for the age group 75–79.

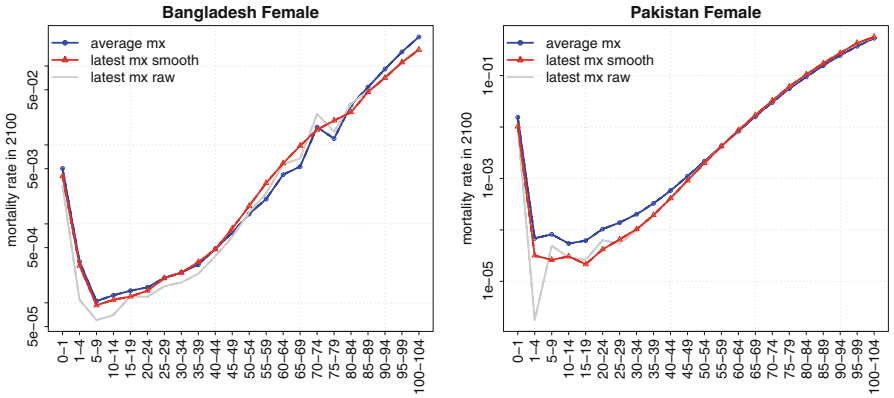

Fig. 15.2 Female age-specific mortality rates for Bangladesh and Pakistan in 2095–2100 projected using three different methods for computing a_x: (1) using an average m_x over time; (2) using the latest smoothed m_x; and (3) using the latest m_x as it is (raw). The y-axis is on the logarithmic scale

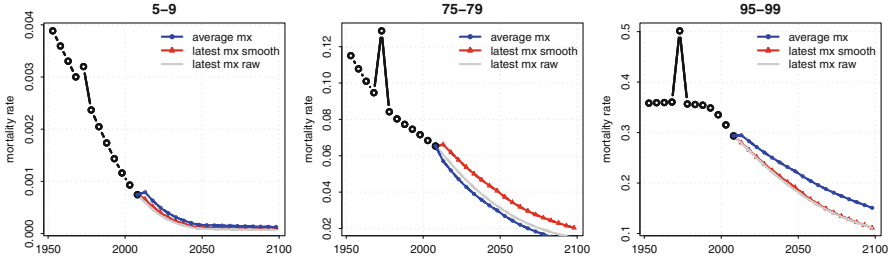

Fig. 15.3 Mortality rates over time for Bangladesh for three different age groups. Line styles correspond to the same methods as in Fig. 15.2

This shows that there is a trade-off between bumpy mortality rates over ages in later projection years and no jump-offs, and smooth mortality rates with no jump-offs. Our solution is to decide on a country-specific basis which method is more appropriate.

15.2.5 Rotated Lee-Carter Method

Li et al. (2013) focused on the fact that in more developed regions, once countries have already reached a high level of life expectancy at birth, the proportional mortality decline decelerates at younger ages and accelerates at old ages. This change in the pace of log mortality decline by age cannot be captured by the original Lee-Carter method, since this constrains the rate of change b_x to be constant over time. They proposed instead rotating the b_x over time to a so-called *ultimate* b_x, denoted by $b_{u,x}$, which is computed as follows.

Let

$$\bar{b}_{15-64} = \frac{1}{10} \sum_{x=15-19}^{60-64} b_x \,.$$

Then

$$b_{u,x} = \begin{cases} \bar{b}_{15-64} & \text{for } x \in \{0-1, 1-4, 5-9, \ldots, 60-64\}, \\ b_x \cdot b_{u,60-64}/b_{65-70} & \text{for } x \in \{65-70, \ldots, 130+\}, \end{cases} \tag{15.7}$$

where $b_{u,x}$ is scaled to sum to unity over all ages.

The rotation is dependent on $e_0(\tau)$, and so the resulting b_x also becomes time-dependent. The rotation finishes at a certain level of life expectancy, denoted by e_0^u. Li et al. (2013) recommended using $e_0^u = 102$. Using the smooth weight function

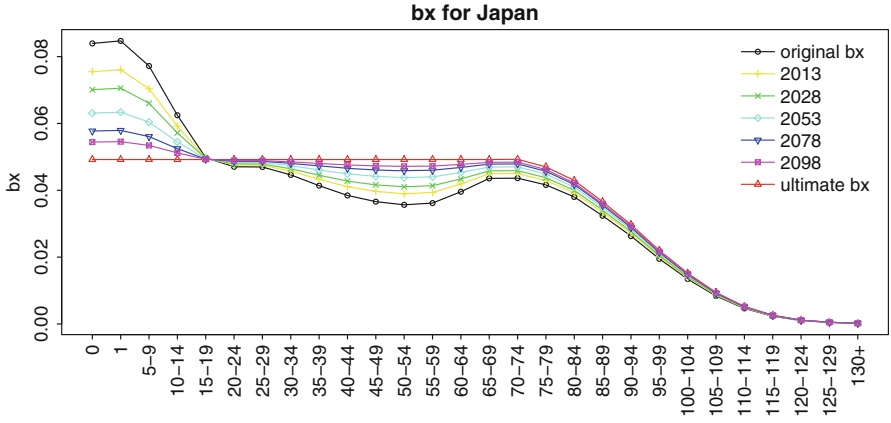

Fig. 15.4 Rotating the parameter b_x over time: data from Japan. The original b_x (*outer curve with circles*) approaches the ultimate $b_{u,x}$ (*outer curve with triangles*) over time starting with the *lightest color* and continuing towards the *darker colors*

$$w(\tau) = \left\{ \frac{1}{2}\left[1 + \sin[\frac{\pi}{2}(2w'(\tau) - 1)]\right]\right\}^{\frac{1}{2}} \quad \text{with} \quad w'(\tau) = \frac{e_0(\tau) - 80}{e_0^u - 80},$$

the rotated b_x at time τ, denoted by $B_x(\tau)$, is derived as:

$$B_x(\tau) = \begin{cases} b_x, & e_0(\tau) < 80, \\ [1 - w(\tau)]\, b_x + w(\tau) b_{u,x}, & 80 \le e_0(\tau) < e_0^u, \\ b_{u,x}, & e_0(\tau) \ge e_0^u. \end{cases} \tag{15.8}$$

Figure 15.4 shows the results for Japan as an example. The original b_x is shown by the black curve with circles. The ultimate $b_{u,x}$, to be reached at life expectancy 102 years, marked by triangles. The remaining curves show the change over time starting with the lightest color and continuing through darker colors towards the ultimate curve.

15.2.6 Computing Life Tables

Step 3 in Algorithm 15.1 calls for matching future $k(\tau)$ to projected $e_0(\tau)$. This is a nonlinear equation in $k(\tau)$. It is solved by an iterative nonlinear procedure in which, for given values of a_x, b_x and $k(\tau)$, a life table is produced, and the resulting life expectancy is computed and compared with the projected $e_0(\tau)$. We used a bisection method to solve the nonlinear equation. This is simple and robust and involves relatively few iterations. It would be possible to use a nonlinear solution

method that is more efficient computationally, but the computational gains would be modest and this could make the method much more complex.

In the process of computing life tables, the conversion of mortality rates $m_x(\tau)$ to probabilities of dying $q_x(\tau)$ follows the approach used by the United Nations to compute abridged life tables. This is computed by the LIFTB function in Mortpak (United Nations 1988, 2013a), where at a given time point the probability of dying for an individual between age x and $x + n$ is:

$$ {}_nq_x = \frac{n * {}_nm_x}{1 + (n - {}_nA_x) * {}_nm_x}, \tag{15.9} $$

with n being the length of the age interval and ${}_nA_x$ being the average number of years lived between ages x and $x + n$ by those dying in the interval. With l_x being the number of survivors at age x, we have

$$ l_{x+n} = l_x(1 - {}_nq_x), \tag{15.10} $$

$$ {}_nd_x = l_x - l_{x+n}, \tag{15.11} $$

$$ {}_nL_x = {}_nA_x l_x - (n - {}_nA_x) l_{x+n}, \tag{15.12} $$

where ${}_nd_x$ denotes the number of deaths between ages x and $x + n$ and ${}_nL_x$ denotes the number of person-years lived between ages x and $x + n$. The expectation of life at age x (in years) e_x is given by

$$ e_x = \frac{T_x}{l_x} \quad \text{with} \quad T_x = \sum_{a=x}^{\infty} {}_nL_a, $$

where T_x is the number of person-years lived at age x and older.

For ages 15 and over, the expression for ${}_nA_x$ is derived from the Greville (1943) approach to calculating age-specific separation factors based on the age pattern of the mortality rates themselves with:

$$ {}_nA_x = 2.5 - \frac{25}{12}({}_nm_x - k), \quad \text{where } k = \frac{1}{10} \log \left(\frac{{}_nm_{x+5}}{{}_nm_{x-5}} \right). $$

For ages 5 and 10, ${}_nA_x = 2.5$ and for ages under 5, values from the Coale and Demeny West region relationships are used for ${}_nA_x$ (Coale and Demeny 1966).[2]

[2]The Coale and Demeny West region formulae are used as follows. When ${}_0m_1 \geqslant 0.107$, then ${}_1A_0 = 0.33$ for males and 0.35 for females; ${}_4A_1 = 1.352$ for males and 1.361 for females. When ${}_1m_0 < 0.107$, ${}_1A_0 = 0.045 + (2.684 \cdot {}_1m_0)$ for males and ${}_1A_0 = 0.053 + (2.800 \cdot {}_1m_0)$ for females; ${}_4A_1 = 1.651 - (2.816 \cdot {}_1m_0)$ for males and ${}_4A_1 = 1.522 - (1.518 \cdot {}_1m_0)$ for females.

15.2.7 Summary of Improved Algorithm

We now summarize the modifications described in the previous sections by proposing an improved algorithm for deriving the age-specific mortality rates m_x for potential use in future probabilistic population projections.

Algorithm 15.2

As before, let $t \in \{1, \ldots, T\}$ and $\tau \in \{T+1, \ldots T_p\}$ denote the observed and projected time periods, respectively. Also, let $g \in \{F, M\}$ be an index to distinguish sex-specific measures.

1. Using the Coherent Kannisto Method from Sect. 15.2.2, extend $m_x(t)$ to higher age categories with $\max(x) = 130+$ for all t.
2. Choose a method to estimate a_x, i.e. one of Eqs. (15.1), (15.5) or (15.6), depending on country specifics.[3] Do the estimation for each sex g, obtaining $\hat{a}_x^g$.
3. Estimate $k(t)$ and b_x using the extended historical $m_x(t)$ and Eqs. (15.2) and (15.3) for $g = M, F$ independently, yielding $\hat{b}_x^g$.
4. Given $\hat{b}_x^M$ and $\hat{b}_x^F$ from Step 3, set $\hat{b}_x = \frac{\hat{b}_x^M + \hat{b}_x^F}{2}$.
5. Compute the ultimate $b_{u,x}$ as in Eq. (15.7).
6. For a combined $e_0(\tau) = \left[e_0^M(\tau) + e_0^F(\tau)\right]/2$ in each trajectory, compute $B_x(\tau)$ as in Eq. (15.8).
7. For a given sex-specific $e_0^g(\tau)$ in each trajectory and the estimated $\hat{a}_x^g$ and $B_x(\tau)$ from the previous steps, solve for future $k_g(\tau)$ numerically using life tables. This yields a nonlinear equation which is solved using the bisection method, as described in Sect. 15.2.6.
   As in Algorithm 15.1, this gives a sample of values of $k_g(\tau)$ for each future time period τ, with one value for each trajectory.
8. For each trajectory, time τ and sex g, compute mortality rates by

$$\log[m_x^g(\tau)] = \hat{a}_x^g + B_x(\tau)k_g(\tau).$$

9. Since the previous step does not comply with Eq. (15.4) and thus can lead to crossovers in high ages, an additional constraint is added:
   If $e_0^M(\tau) < e_0^F(\tau)$ then

$$m_x^M(\tau) = \max[m_x^M(\tau), m_x^F(\tau)] \text{ for } x \geq 100.$$

Figure 15.5 shows the resulting probabilistic projection of $m_x(\tau)$ for the period 2095–2100 for both sexes in two selected countries. In addition to the marginal distribution for Kazakhstan in the right panel of Fig. 15.5, its joint distribution for males and females is shown in Fig. 15.6 on a logarithmic scale. Points below the $x = y$ solid line indicate crossovers in the individual trajectories. It can be seen that only a few trajectories experience crossovers when mortality is low, i.e. in young ages, suggesting a low (but non-zero) probability for such an event. There are no

[3] In the bayesPop package this country-specific set of options is controlled through two dummy variables in the `vwBaseYear2012` dataset: (1) whether the most recent estimate of age mortality pattern should be used (LatestAgeMortalityPattern) and (2) whether it should be smoothed (SmoothLatestAgeMortalityPattern). See `help(vwBaseYear2012)` in R.

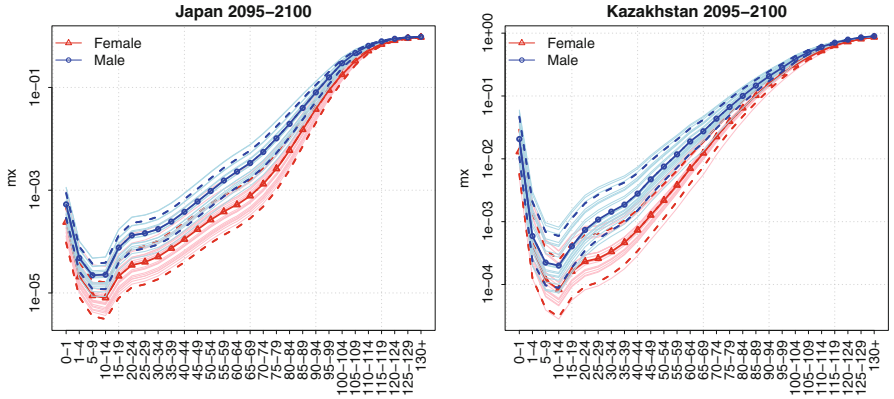

Fig. 15.5 Probabilistic projection of age-specific mortality rates for Japan (*left panel*) and Kazakhstan (*right panel*) in the time period 2095–2100. Both plots show the marginal distributions for males and females where the *dashed lines* mark the 80 % probability intervals and the *solid lines* are 20 randomly sampled trajectories for each sex. The *y*-axis is on the logarithmic scale

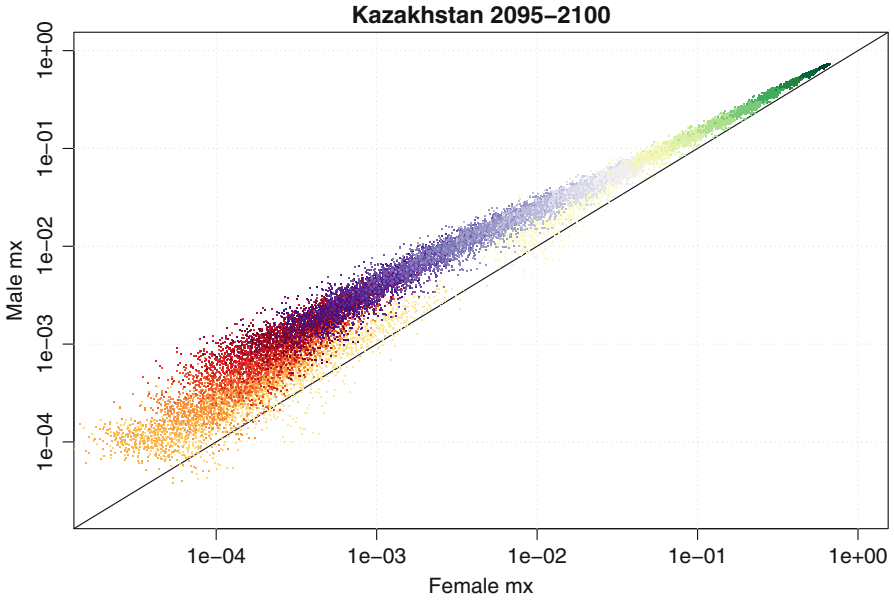

Fig. 15.6 The joint predictive distribution of mortality rates for females and males for Kazakhstan in 2095–2100. It shows mortality rates from all age groups. Age groups are distinguished by color in the online version. Both axes are on the logarithmic scale. There are 1000 points per age group

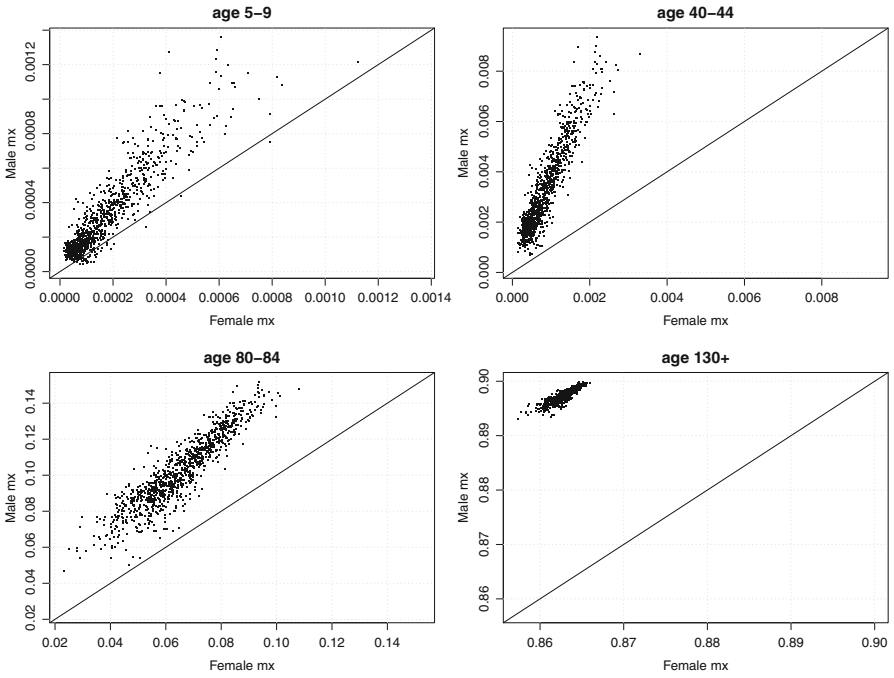

Fig. 15.7 The joint predictive distribution of future age-specific mortality rates for females and males for Kazakhstan in 2095–2100 for four individual age groups. In all panels, 1000 points are shown and all axes are on a normal scale

crossovers for high mortality, i.e. at old ages. We observed similar results for most countries. Figure 15.7 shows the same joint distribution for selected age groups on a normal scale.

15.2.7.1 Exceptions

For about 50 countries, insufficient detailed data about mortality by age and sex are available between 1950 and 2010 (United Nations 2013c). Therefore, the age patterns of mortality are based on model life tables (e.g., Coale-Demeny). For these countries a model b_x associated with one of the regional model life tables is used (see Table 2 page 18 in Li and Gerland 2011).[4]

In addition, for about 40 countries with a generalized HIV/AIDS epidemic, age patterns of mortality since the 1980s have been affected by the impact

[4]In the bayesPop package this country-specific set of options is controlled through two variables in the `vwBaseYear2012` dataset: (1) the type of age mortality pattern used for the estimation period (AgeMortalityType with the option "Model life tables") and (2) the specific mortality pattern used (AgeMortalityPattern with options like "CD West").

of AIDS mortality (especially before the scaling up of antiretroviral treatment starting in 2005). For these countries the application of the conventional Lee-Carter approach is inappropriate.[5] Instead, we introduce a modification where steps 2–6 in Algorithm 15.2 are replaced by the following steps:

1. Start with the most recent a_x (affected by impact of HIV/AIDS on mortality) and smooth it as in Eq. (15.6), obtaining a_x^s.
2. Compute an *ultimate* (or "AIDS-free" target) a_x, denoted by a_x^u, which is a smoothed average of historical $\log(m_x)$ up to 1985 (i.e., prior to the start of the impact caused by HIV/AIDS on mortality), denoted by a_x^v:

$$a_x^v = \frac{\sum_{t=1}^{T_u} \log[m_x(t)]}{T_u} \text{ with } T_u \text{ corresponding to 1985}$$
$$a_x^u = \text{smooth}_x\{a_x^v\} \text{ with } a_{0-1}^u = a_{0-1}^v \tag{15.13}$$

3. For each x interpolate from a_x^s to a_x^u assuming that in the long run the excess mortality due to the HIV/AIDS epidemic disappears (or reaches a very low endemic level with negligible mortality impact) both as a result of decreased HIV prevalence, improved access to treatment and survival with treatment.
4. During the projections, pick an $a_x(\tau)$ by moving along the interpolated line of the corresponding x, so that a_x^u is reached by 2100.
5. As above, b_x is associated with one of the regional model life tables.

An example of the resulting projected median age-specific mortality rates for Botswana, a country with a generalized HIV/AIDS epidemic, is shown in Fig. 15.8.

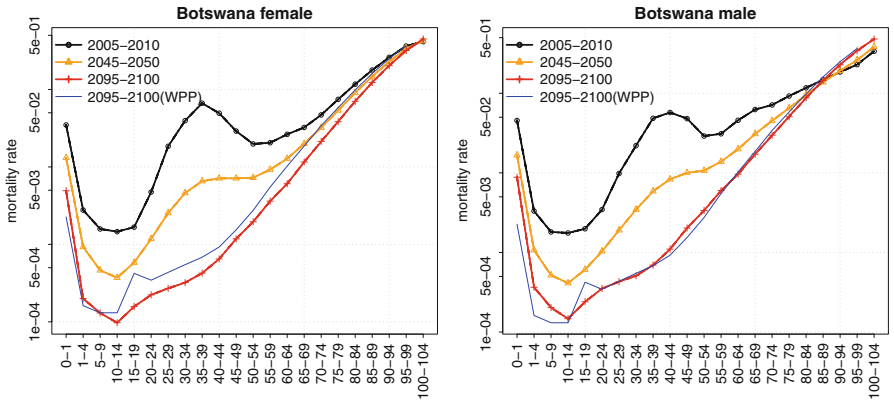

Fig. 15.8 Projected age-specific mortality rates for Botswana, a country with a generalized HIV/AIDS epidemic. The *y*-axis is on the logarithmic scale

[5]In the bayesPop package this specific-set of countries are identified through a dummy variable (WPPAIDS) in the `vwBaseYear2012` dataset.

There has been recent progress in the modelling of age patterns of mortality for countries with generalized HIV/AIDS (Sharrow et al. 2014). This could provide additional options to better incorporate the uncertainty about future HIV prevalence, expanded access to treatment, underlying age mortality patterns, and their interaction on overall mortality by age into probabilistic population projections. Further calibration and validation of these models using empirical estimates from cohort studies (Zaba et al. 2007; Reniers et al. 2014) will be important in this context.

15.3 Age-Specific Fertility Rates for Probabilistic Population Projections

15.3.1 WPP 2012 Method of Projecting Age-Specific Fertility Rates

The United Nations probabilistic population projections released in 2014 (Gerland et al. 2014) used a set of projected age-specific fertility rates for each country obtained by combining probabilistic projections of the total fertility rate with deterministic projections of age patterns of fertility as used in the 2012 revision of the World Population Prospects (United Nations 2014).

For high-fertility and medium-fertility countries, future age patterns of fertility were obtained by interpolating linearly between a starting proportionate age pattern of fertility and a target model pattern. The target model pattern was chosen from among 15 proportionate age patterns of fertility, with mean age at childbearing varying between 24 and 28.5 years. The target pattern was held constant once the country reaches its lowest fertility level, or by 2045–2050 onward.

For low fertility countries, a similar approach was used. It projected future age-specific fertility patterns by assuming that they would reach a target model pattern by 2025–2030. This target was chosen from among five target age patterns of fertility either for the market economies of Europe (with mean age of childbearing varying between 28 and 32 years) or for countries with economies in transition (with mean age of childbearing varying between 26 and 30 years). Once the model pattern was reached, it was assumed to remain constant until the end of the projection period. In some instances, a modified Lee-Carter approach (Li and Gerland 2009) was used to extrapolate the most recent set of proportionate age-specific fertility rates using the rates of change from country-specific historical trends.

All the trajectories making up the probabilistic projection of fertility for a given country used the same age pattern of fertility. The choice of target pattern of fertility for a given country, from among the set of model patterns considered, was driven by country-specific expert opinion about future trends and normative assumptions. No global or regional convergence in age patterns of fertility was imposed.

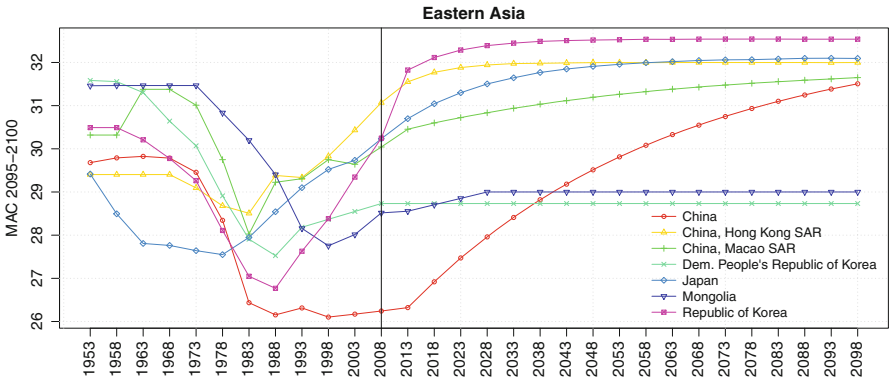

Fig. 15.9 Example of projected Mean Age of Childbearing (MAC) for countries in Eastern Asia in WPP 2012

Figure 15.9 shows the results of the projections for the Mean Age of Childbearing (MAC) for countries in Eastern Asia from the 2012 Revision of the World Population Prospects.

Overall, the method for projecting age-specific patterns of fertility in the 2012 Revision (as well as in previous revisions) has several limitations. First, no global or regional convergence has been imposed despite the overall convergence in total fertility rates observed in the projection period up to 2100. Second, the time point when the target age-specific pattern is reached is not related to the projected total fertility rates. Third, expert assumptions on the target age pattern and method used for individual countries introduce diversity in the age-specific trends that are difficult to explain (see Fig. 15.9—Mongolia and Democratic People's Republic of Korea were done by Analyst 1, all other countries by Analyst 2). Finally, since the analysts have used at least two different methods and 25 target age patterns of fertility, the documentation of the decisions made for individual countries have been challenging.

15.3.2 Convergence Method for Projecting Age-Specific Fertility Rates

We now propose a new method for projecting age-specific fertility rates, to overcome some of the limitations of the existing method used in WPP 2012. This builds on the approach adopted in sets of projections of married or in-union women of reproductive age (MWRA) (United Nations 2013b). Beginning from the most recent observation of the age pattern of fertility in the base period of projection, the projected age patterns of fertility are based on the past national trend combined with the trend towards the global model age pattern of fertility. The projection method

is implemented on the proportionate age-specific fertility rates (PASFR) covering seven age groups from 15–19 to 45–49. The final projection of PASFRs for each age group is a weighted average of two preliminary projections:

(a) the first preliminary projection, assuming that the PASFRs converge to the global model pattern, see Sect. 15.3.2.1; and
(b) the second preliminary projection, assuming the observed national trend in PASFRs continues into the indefinite future, see Sect. 15.3.2.2.

The method is applied to all TFR trajectories from 2014 PPP.

We now define the preliminary projections that constitute our overall projection. We use different notation than in Sect. 15.2, so the same symbol may be used to denote different quantities in the two sections.

15.3.2.1 Trend Towards the Global Model Pattern

Let t_r denote the base period of a projection and t_g the year when the global model pattern is reached. For $t_r < t < t_g$, the proportion of the interval $[t_r, t_g]$ that has elapsed at time t is

$$\tau_t = (t - t_r)/(t_g - t_r).$$

Section 15.3.2.4 below gives details about how to estimate t_g.

Let p_r denote PASFR at the base period t_r, and let p_g denote PASFR of the global model pattern.[6] The projections at time t of PASFR towards the global model pattern, denoted by p_t^I, is obtained by:

$$\text{logit}(p_t^I) = \text{logit}(p_r) + \tau_t \left[\text{logit}(p_g) - \text{logit}(p_r)\right] \tag{15.14}$$

Then p_t^I is renormalized so that it sums to unity for all time periods t.

15.3.2.2 Continuing of Observed National Trend

Let T denote the number of 5-year periods over which the model is fitted. Then t_{r-T} is the starting time period of the estimation and $p_{(r-T)}$ is PASFR at t_{r-T}. p_t^{II} is the

[6] In the bayesPop package the global model pattern is created as an average of most recent PASFRs for a set of countries (selected through a dummy variable in the `vwBaseYear2012` dataset). For the purpose of the current analysis, the low fertility countries selected have already reached their Phase III and represent later childbearing patterns with mean age at childbearing close to or above 30 years in 2010–2015: Austria, the Czech Republic, Denmark, France, Germany, Japan, the Netherlands, Norway and the Republic of Korea. The specification of the countries used for the global model pattern can be changed in input file.

projected PASFR at time t, assuming the past trend was to continue into the future under the following rule:

$$\text{logit}(p_t^{II}) = \text{logit}(p_r) + \frac{t - t_r}{t_r - t_{r-T}} [\text{logit}(p_r) - \text{logit}(p_{r-T})] \quad (15.15)$$

As above, p_t^{II} should be scaled to sum to unity for all t. Note that in our implementation we use $T = 3$.

15.3.2.3 Resulting Projection

Projected PASFR at time t, p_t, is calculated as:

$$\text{logit}(p_t) = \tau_t \cdot \text{logit}(p_t^I) + (1 - \tau_t) \text{logit}(p_t^{II}) \quad (15.16)$$

Resulting p_t is renormalized to sums to unity for all time periods t.

15.3.2.4 Estimating the Time Period of Reaching Global Pattern

We assume that the transition from the most recent age pattern of fertility to the global model age pattern of fertility is dependent on the timing when TFR enters Phase III, i.e. when the fertility transition is completed and the country reaches low fertility. For the countries in Phase III, a time series model to project TFR was used that assumed that in the long run fertility would approach and fluctuate around country-specific ultimate fertility levels based on a Bayesian hierarchical model (Raftery et al. 2014a). The time series model uses the empirical evidence from low-fertility countries that have experienced fertility increases from a sub-replacement level after a completed fertility transition. At the same time, based on the empirical evidence on the postponement of childbearing in low-fertility countries, profound shifts to later start of childbearing and an increase in the mean age of childbearing are still taking place several periods after the start of Phase III (see Fig. 15.10). The timing and speed of the postponement of childbearing in Phase III is country-specific and in this chapter we implement the assumption that the transition to later childbearing pattern is completed when total fertility approaches country-specific ultimate fertility levels.

To be more specific, we assume that the time t_g of a completion of the transition to a global model pattern corresponds to the time point t_u, when TFR reaches the ultimate fertility level of that country. In probabilistic projections of TFR, we approximate the ultimate fertility level, denoted by f_u, by the median TFR in the last projection period t_e, e.g. $t_e = 2095$–2100, if TFR is in Phase III:

$$\hat{f}_u = \text{median}_i [f_i(t_e)] \quad (i \text{ denotes trajectories}) \quad (15.17)$$

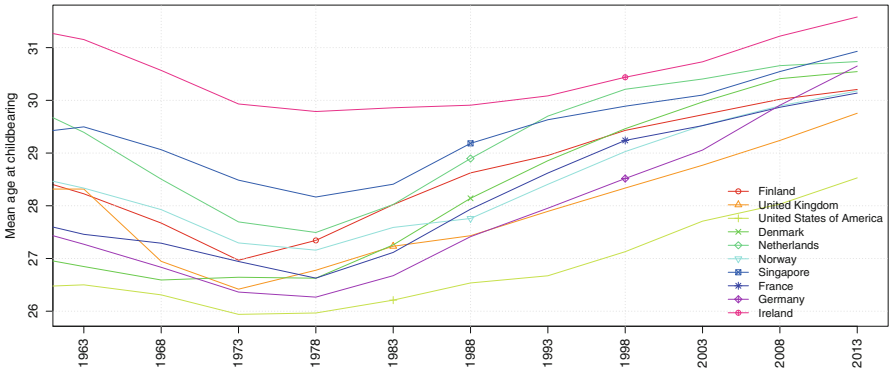

Fig. 15.10 Trends in mean age at childbearing in countries with the start of Phase III of fertility decline before 2000. *Symbols* mark the time period when the country entered Phase III

Then for each TFR trajectory, t_u is the earliest time period, at which the TFR is larger or equal to $\hat{f}_u$:

$$t_u = \min\{t : f(t) \geqslant \hat{f}_u \text{ and } t > t_{P3}\} \tag{15.18}$$

where t_{P3} denotes the start of Phase III. For the estimation of t_g, we will now distinguish two cases, depending if t_{P3} is smaller or larger than the end period t_e.

Case 1: $t_{P3} < t_e$

In this case, t_{P3} is either observed ($t_{P3} \leqslant t_r$) or projected within the projecting period ($t_r < t_{P3} < t_e$). In both cases, if t_u exists,

$$t_g = \max(t_u, t_r + 10)\,. \tag{15.19}$$

This includes a situation where $f(t) \geqslant \hat{f}_u$ for $t \leqslant t_r$. In such a case, the global pattern is reached quickly, namely in two 5-year periods.

If $f(t) < \hat{f}_u$ for all $t_r \leqslant t \leqslant t_e$, then t_u does not exist. In such a case, t_g is set to the end of the projection period, but at least five 5-year periods after t_{P3}:

$$t_g = \max(t_e, t_{P3} + 25) \tag{15.20}$$

Case 2: $t_e \leqslant t_{P3}$

In this case, t_{P3} is unknown, i.e. the TFR trajectory has not reached Phase III at t_e. Thus, we will make an estimate of t_{P3}, denoted by $\hat{t}_{P3}$, and then simply apply

$$t_g = \hat{t}_{P3} + 25\,. \tag{15.21}$$

If the TFR at t_e is low, namely $f(t_e) \leqslant 1.8$, we assume that $\hat{t}_{P3} = t_e$. Otherwise, we approximate t_{P3} by a linear extrapolation of TFR from the last four time periods and determine when such line reaches 1.8, with an upper limit of $\hat{t}_{P3} = t_e + 50$.

15.3.2.5 Exception for Late Childbearing Pattern

Since trajectories for some countries have already observed or – as projected by the algorithm described above – will in near future reach higher MAC than the MAC associated with the global model pattern, we assume that for a given country's trajectory once the maximum MAC is reached in the convergence period the associated PASFR pattern is kept constant for the remaining projection periods. This assumption enables to keep trajectory-specific patterns of late childbearing for trajectories after the Phase III, thus already with low total fertility (see Fig. 15.11 for example of the Czech Republic). Note that this rule is applied only in Case 1 above.

15.3.3 Results of the Convergence Method Applied to Probabilistic Projections

For the 2012 Revision, age-specific fertility estimates are based on empirical data for all countries of the world for the period up to 2010 (or up to 2010–2015 for 37 countries with empirical data up to 2011 or 2012; Gerland et al. 2014). Using the probabilistic projections of TFR, each TFR trajectory has a specific start of Phase III and therefore the timing of convergence to the global model pattern is trajectory-specific. This yields a set of trajectories of PASFR (although not probabilistic) which in turn, when combined with the probabilistic TFR, yield probabilistic projection of age-specific fertility rates.

Figure 15.11 shows an example of the results for PASFR in Niger, Bangladesh and the Czech Republic for selected age groups over time. Figure 15.12 shows an example of the probabilistic results of age-specific fertility rates for Ethiopia, Nepal and Japan at the end of projection period in 2095–2100.

Figure 15.13 shows the development of PASFR for Uganda, India and Germany over time from 2005–2010 to 2095–2100. Here, the methodology was applied to the deterministic projection of TFR from WPP 2012.

In Fig. 15.9 we showed projections of MAC from WPP 2012. This can be compared to Fig. 15.14 where the same measure is shown after applying the new methodology to the TFR of WPP 2012.

Overall, the new method we propose improves on the current methodology in several ways. First, in the very long term (after 2100) the age patterns of fertility are converging to one global pattern, while retaining specific late childbearing patterns

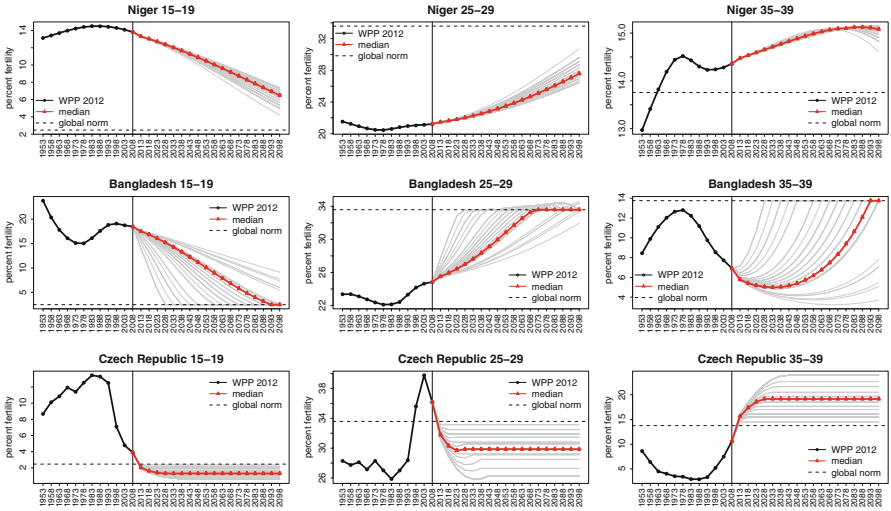

Fig. 15.11 Proportionate age-specific fertility rates (PASFR) by time for age groups 15–19, 25–29 and 35–39 in Niger, Bangladesh and the Czech Republic. Projected median of PASFR approaches global model pattern of PASFR (*dashed line*). The *solid grey lines* are trajectories that correspond to different starting periods for Phase III; they do not represent random samples from a predictive probability distribution

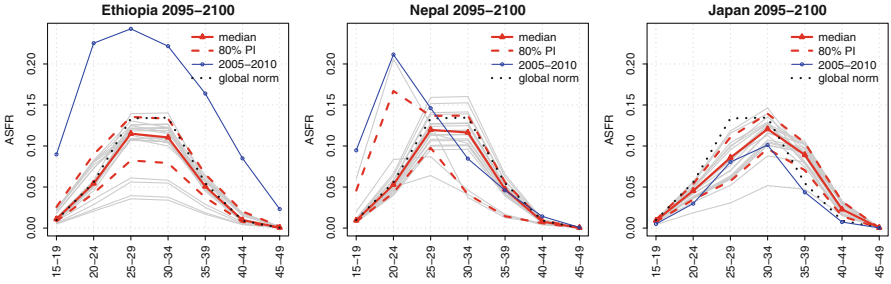

Fig. 15.12 Probabilistic projection of age-specific fertility rates for Ethiopia (*left panel*), Nepal (*middle panel*) and Japan (*right panel*) in the time period 2095–2100. The marginal distribution for age-specific fertility rates (*red lines*) where the *dashed lines* mark the 80 % probability intervals and the *solid grey lines* are randomly sampled trajectories are compared to age-specific fertility rates in the time period 2005–2010 (*blue line*) and to the global model pattern applied to median projection of total fertility for the world in 2095–2100 (*black dotted line*)

for several countries that reach such patterns in the current period or in the near future. Second, the projections of the age pattern of fertility are now linked to projections of the total fertility rate. Finally, for each probabilistic trajectory, the time when the target age pattern is reached depends on the trajectory-specific total fertility rate.

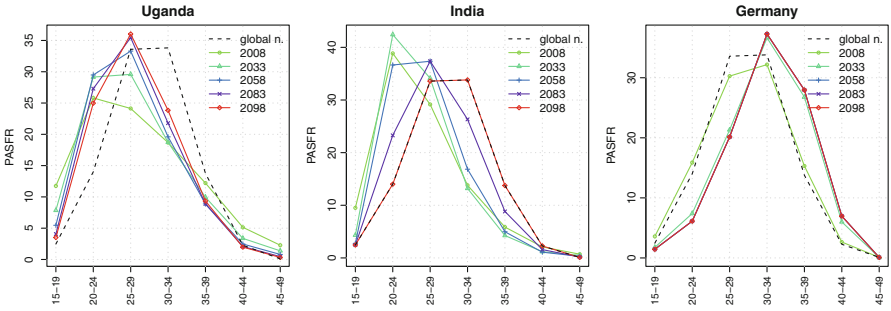

Fig. 15.13 Proportionate age-specific fertility rates (PASFR) by age over time for selected countries

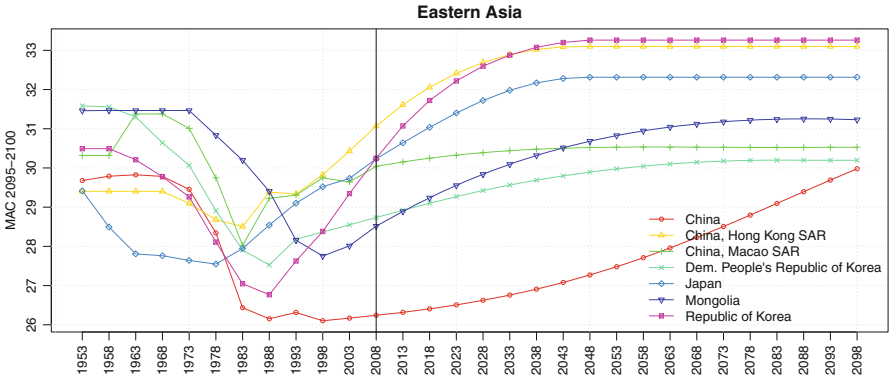

Fig. 15.14 Example of projected MAC for countries in Eastern Asia after applying the proposed methodology

15.4 Discussion

We have described the methods used for converting projected life expectancies at birth and total fertility rates to age-specific mortality and fertility rates in the UN's 2014 probabilistic population projections. We have identified some limitations of these methods and have proposed several improvements to overcome them. These include a new coherent Kannisto method to avoid crossovers in mortality rates between the sexes at very high ages. They also include the application of the coherent Lee-Carter method to avoid crossovers in mortality rates between the sexes at lower ages, methods for avoiding jump-off bias, and the rotated Lee-Carter method to reflect the fact that at high life expectancies, mortality rates tend to decline faster at higher than at lower ages.

It should be noted that the 2014 PPP takes account of uncertainty about the overall level of fertility as measured by the TFR, and also about the overall level of mortality as measured by e_0. Conditional on TFR and e_0, however, the projected

vital rates are deterministic. There is thus a missing component of uncertainty, and it would be desirable to extend the methods used to take account of this, particularly of uncertainty about the future mean age at childbearing (Ediev 2013).

Acknowledgements This research was supported by NIH grants R01 HD054511 and R01 HD070936. The views expressed in this article are those of the authors and do not necessarily reflect those of NIH or the United Nations. The authors are grateful to the editor for very helpful comments.

References

Alders, M., Keilman, N., & Cruijsen, H. (2007). Assumptions for long-term stochastic population forecasts in 18 European countries. *European Journal of Population, 23*, 33–69.

Alho, J. M., Alders, M., Cruijsen, H., Keilman, N., Nikander, T., & Pham, D. Q. (2006). New forecast: Population decline postponed in Europe. *Statistical Journal of the United Nations Economic Commission for Europe, 23*, 1–10.

Alho, J. M., Jensen, S. E. H., & Lassila, J. (2008). *Uncertain demographics and fiscal sustainability*. Cambridge/New York: Cambridge University Press.

Alkema, L., Raftery, A. E., Gerland, P., Clark, S. J., Pelletier, F., Buettner, T., & Heilig, G. K. (2011). Probabilistic projections of the total fertility rate for all countries. *Demography, 48*, 815–839.

Booth, H., Hyndman, R. J., Tickle, L., & de Jong, P. (2006). Lee-Carter mortality forecasting: A multi-country comparison of variants and extensions. *Demographic Research, 15*, 289–310.

Bos, E., Vu, M. T., Massiah, E., & Bulatao, R. (1994). *World population projections 1994–95: Estimates and projections with related demographic statistics*. Baltimore: Johns Hopkins University Press for the World Bank.

Coale, A. J., & Demeny, P. G. (1966). *Regional model life tables and stable populations*. Princeton: Princeton University Press.

Ediev, D. M. (2013). *Comparative importance of the fertility model, the total fertility, the mean age and the standard deviation of age at childbearing in population projections*. Presented at the Meeting of the International Union for the Scientific Study of Population, Busan. http://iussp.org/sites/default/files/event_call_for_papers/TF%20MS%20SD_what%20matters_StWr.pdf

Gerland, P., Raftery, A. E., Ševčíková, H., Li, N., Gu, D., Spoorenberg, T., Alkema, L., Fosdick, B. K., Chunn, J. L., Lalic, N., Bay, G., Buettner, T., Heilig, G. K., & Wilmoth, J. (2014). World population stabilization unlikely this century. *Science, 346*, 234–237.

Greville, T. N. (1943). Short methods of constructing abridged life tables. *The Record of the American Institute of Actuaries, XXXII, 1*, 29–42.

Keyfitz, N. (1981). The limits of population forecasting. *Population and Development Review, 7*, 579–593.

Lee, R. D., & Carter, L. (1992). Modeling and forecasting the time series of US mortality. *Journal of the American Statistical Association, 87*, 659–671.

Lee, R. D., & Miller, T. (2001). Evaluating the performance of the Lee-Carter method for forecasting mortality. *Demography, 38*, 537–549.

Lee, R. D., & Tuljapurkar, S. (1994). Stochastic population forecasts for the United States: Beyond high, medium, and low. *Journal of the American Statistical Association, 89*, 1175–1189.

Leslie, P. H. (1945). On the use of matrices in certain population dynamics. *Biometrika, 33*, 183–212.

Li, N., & Gerland, P. (2009). *Modelling and projecting the postponement of childbearing in low-fertility countries*. Presented at the XXVI IUSSP International Population Conference. iussp2009.princeton.edu/papers/90315

Li, N., & Gerland, P. (2011). *Modifying the Lee-Carter method to project mortality changes up to 2100*. Presented at the Annual Meeting of Population Association of America. http://paa2011.princeton.edu/abstracts/110555

Li, N., & Lee, R. D. (2005). Coherent mortality forecasts for a group of populations: An extension of the Lee-Carter method. *Demography, 42*, 575–594.

Li, N., Lee, R. D., & Gerland, P. (2013). Extending the Lee-Carter method to model the rotation of age patterns of mortality decline for long-term projections. *Demography, 50*, 2037–2051.

Lutz, W., & Samir, K. C. (2010). Dimensions of global population projections: What do we know about future population trends and structures? *Philosophical Transactions of the Royal Society B, 365*, 2779–2791.

Lutz, W., Sanderson, W. C., & Scherbov, S. (1996). Probabilistic population projections based on expert opinion. In Lutz, W. (Ed.), *The future population of the world: What can we assume today*? (pp. 397–428). London: Earthscan Publications Ltd. Revised 1996 edition.

Lutz, W., Sanderson, W. C., & Scherbov, S. (1998). Expert-based probabilistic population projections. *Population and Development Review, 24*, 139–155.

Lutz, W., Sanderson, W. C., & Scherbov, S. (2004). *The end of world population growth in the 21st century: New challenges for human capital formation and sustainable development*. Sterling: Earthscan.

National Research Council. (2000). *Beyond six billion: Forecasting the world's population*. Washington, DC: National Academy Press.

Pflaumer, P. (1988). Confidence intervals for population projections based on Monte Carlo methods. *International Journal of Forecasting, 4*, 135–142.

Preston, S. H., Heuveline, P., & Guillot, M. (2001). *Demography: Measuring and modeling population processes*. Malden: Blackwell.

Raftery, A. E., Li, N., Ševčíková, H., Gerland, P., & Heilig, G. K. (2012). Bayesian probabilistic population projections for all countries. *Proceedings of the National Academy of Sciences, 109*, 13915–13921.

Raftery, A. E., Chunn, J. L., Gerland, P., & Ševčíková, H. (2013). Bayesian probabilistic projections of life expectancy for all countries. *Demography, 50*, 777–801.

Raftery, A. E., Alkema, L., & Gerland, P. (2014a). Bayesian population projections for the United Nations. *Statistical Science, 29*, 58–68.

Raftery, A. E., Lalic, N., & Gerland, P. (2014b). Joint probabilistic projection of female and male life expectancy. *Demographic Research, 30*, 795–822.

Reniers, G., Slaymaker, E., Nakiyingi-Miiro, J., Nyamukapa, C., Crampin, A. C., Herbst, K., Urassa, M., Otieno, F., Gregson, S., Sewe, M., Michael, D., Lutalo, T., Hosegood, V., Kasamba, I., Price, A., Nabukalu, D., Mclean, E., Zaba, B., & Network, A. (2014). Mortality trends in the era of antiretroviral therapy: Evidence from the network for analysing longitudinal population based HIV/AIDS data on Africa (ALPHA). *AIDS, 28*, S533–S542.

Ševčíková, H., & Raftery, A. E. (2014). *bayesPop: Probabilistic population projection*. R package version 5.4-0.

Ševčíková, H., Raftery, A. E., & Gerland, P. (2014). *Bayesian probabilistic population projections: Do it yourself*. Presented at the Annual Meeting of Population Association of America. http://paa2014.princeton.edu/abstracts/141301

Sharrow, D. J., Clark, S. J., & Raftery A. E. (2014). Modeling age-specific mortality for countries with generalized HIV epidemics. *PLoS One, 9*, e96447.

Stoto, M. A. (1983). The accuracy of population projections. *Journal of the American Statistical Association, 78*, 13–20.

Thatcher, A. R., Kannisto, V., & Vaupel, J. W. (1998). *The force of mortality at ages 80 to 120* (Volume 5 of odense monographs on population aging series). Odense: Odense University Press.

Tuljapurkar, S., & Boe, C. (1999). Validation, probability-weighted priors, and information in stoachastic forecasts. *International Journal of Forecasting, 15*, 259–271.

United Nations. (1988). *MortPak – The United Nations software package for mortality measurement. Bach-oriented software for the mainframe computer* (ST/ESA/SER.R/78). New York: United Nations. Available at http://www.un.org/esa/population//publications/MortPak_SoftwarePkg/MortPak_SoftwarePkg.htm

United Nations. (2011). *World population prospects: The 2010 revision*. Population Division, Deptartment of Economic and Social Affairs, United Nations, New York.

United Nations. (2013a). MortPak for Windows Version 4.3 – The United Nations software package for demographic mortality measurement.

United Nations. (2013b). *National, regional and global estimates and projections of the number of women aged 15 to 49 who are married or in a union, 1970–2030* (Technical paper 2013/2). Population Division, Deptartment of Economic and Social Affairs, United Nations, New York.

United Nations. (2013c). *World population prospects: The 2012 revision – online and DVD edition – data sources and meta information (POP/DB/WPP/Rev.2012/F0-2)*. Population Division, Deptartment of Economic and Social Affairs, New York.

United Nations. (2014). *World population prospects: The 2012 revision, methodology of the United Nations population estimates and projections. ESA/P/WP.235*. Population Division, Deptartment of Economic and Social Affairs, United Nations, New York.

U. S. Census Bureau (2009). International data base: Population estimates and projections methodology. Available at http://www.census.gov/ipc/www/idb/estandproj.pdf

Whelpton, P. K. (1928). Population of the United States, 1925–1975. *American Journal of Sociology, 31*, 253–270.

Whelpton, P. K. (1936). An empirical method for calculating future population. *Journal of the American Statistical Association, 31*, 457–473.

Wilmoth, J. R., Andreev, K., Jdanov, D., & Glei, D. A. (2007). Methods protocol for the Human Mortality Database. Online publication of the Human Mortality Database. http://www.mortality.org/Public/Docs/MethodsProtocol.pdf

Zaba, B., Marston, M., Crampin, A. C., Isingo, R., Biraro, S., Barnighausen, T., Lopman, B., Lutalo, T., Glynn, J. R., & Todd, J. (2007). Age-specific mortality patterns in HIV-infected individuals: A comparative analysis of African community study data. *Aids, 21*(6), S87–S96.